Non-Gaussian estimation of a two-vortex flow using a Lagrangian sensor guided by output feedback control

Francis D. Lagor, Amy Davis, Kayo Ide, and Derek A. Paley

Abstract— **This paper considers the closed-loop navigation of a hypothetical ocean-sampling vehicle in the presence of an idealized ocean-eddy pair. This problem embodies many of the challenges of spatiotemporal ocean sampling using minimally actuated Lagrangian sensors. We extend our existing guidance strategy known as the Boundary-Touring Algorithm (BTA) to steer a self-propelled vehicle to a unique streamline in a two-vortex flow. The Gaussian Mixture Kalman Filter (GMKF) provides non-Gaussian state estimation of the vortex parameters based on linear observations of Lagrangian sensor position. Taken together, BTA and GMKF constitute a novel guidance framework for adaptive, Lagrangian data assimilation. Results from numerical experiments are presented for a drifting vehicle, a controlled vehicle that has knowledge of the flow field, and a controlled vehicle that navigates based on its own flow field estimate using the BTA/GMKF framework.**

I. INTRODUCTION

The problem of spatiotemporal sampling for environmental monitoring contains unique challenges in the oceanographic setting. Ocean-sampling platforms must cover large distances and endure extended deployments. For example, the Argo system, which is a state-of-the-art ocean-observing network, consists of floats that make vertical-profile dives, but otherwise drift passively with the flow [1]. The next ocean-observing network may contain platforms such as gliders, which are vehicles capable of steering and buoyancy-driven propulsion, or other self-propelled, long-endurance vehicles [2],[3]. Utilizing such platforms and their Lagrangian data (i.e., time-series measurements of vehicle position), autonomous control algorithms may exploit flow-field forecasts by using underlying currents for transport and uncertainty reduction.

Previous work [4] identified the importance of coherent structures in the flow field for understanding spatial transport and sampling coverage. Works in the field of Lagrangian data assimilation have optimized the launch site of passively drifting vehicles (e.g., see [5]). Other works have considered energy-optimal [6] and time-optimal [7] paths for continuously self-propelled vehicles. However, a comprehensive framework for adaptive data-driven estimation of a flow field by a hypothetical vehicle with intermittent actuation does not yet exist. Intermittent actuation extends endurance and permits targeted sampling of desirable regions.

This paper focuses on the development of an autonomous estimation and control framework to enable a sampling platform capable of steering and flow-relative propulsion to estimate a potential flow field with unknown parameters. The potential-flow model selected for testing the framework is a two-point-vortex system. The periodic motion of two point vortices in relative equilibrium (e.g., rotating together at a constant rate) represents an idealized model of a naturally-occurring ocean eddy pair. Further, it is a demonstrative problem for studying autonomous navigation, because when viewed from a co-rotating frame, this system contains invariant sets that can be used to study the role of coherent structures in navigation and flow-field estimation.

One key component in the control framework is an observability-based navigation algorithm, which relies on the prior finding [3] that boundaries of invariant sets in a divergence-free flow are highly observable due the eventual distinction of neighboring trajectories by an upstream saddle point. We review our algorithm, known as the Boundary-Touring Algorithm (BTA), previously proposed for touring invariant set boundaries, which yields high observability of the flow field parameters [3]. We extend the BTA by modeling the vehicle as a self-propelled particle in a flow and develop a steering control law that drives it to a unique, closed streamline. The steering control law represents a novel application of an existing transformation of the vehicle speed and heading relative to the flow [8] and an existing flow-free steering algorithm [9] to a time-invariant flow field that is well-described by a streamfunction. We ensure that the vehicle drives to a unique streamline by implementing a steering control built around a Bertrand family of curves extended from the streamline. The streamline steering control also uses a virtual cylinder to smooth boundaries of invariant sets near saddle points.

Another key component in the control framework is a non-Gaussian state estimator—the Gaussian Mixture Kalman Filter (GMKF)—that accommodates nonlinear dynamics and non-Gaussian probability densities by approximating them with a mixture of Gaussians selected to minimize the Bayesian Information Criterion, thereby yielding the simplest (based on the number of parameters) fit of a Gaussian mixture to the data [10]. The BTA and GMKF are combined in a novel, guided-Lagrangian data-assimilation framework for estimation of an unknown flow field using feedback of vehicle position measurements. The BTA drives the vehicle

Francis D. Lagor is a graduate student in the Department of Aerospace Engineering, University of Maryland, College Park, MD 20742.

Amy Davis is an undergraduate student at Covenant College, Lookout Mountain, GA 30750.

Kayo Ide is an Associate Professor in the Department of Atmospheric and Oceanic Science, University of Maryland, College Park, MD 20742.

Derek A. Paley is the Willis H. Young Jr. Associate Professor of Aerospace Engineering Education in the Department of Aerospace Engineering and the Institute for Systems Research, University of Maryland, College Park, MD 20742. dpaley@umd.edu

This research is supported by the National Science Foundation under grants PHY-1461089 and CMMI-1362837.

along a trajectory of high observability using the best estimate of the flow-field parameters. The GMKF assimilates Lagrangian data (after accounting for the vehicle's own control effort) to produce more informed estimates of the parameters, thus yielding a new flow-field map for the BTA to tour.

The contributions of this work are as follows: (1) a steering control for the Boundary-Touring Algorithm that drives a self-propelled vehicle to a unique, closed streamline of the two-vortex flow field; (2) implementation of a Gaussian Mixture Kalman Filter (GMKF) with direct state propagation to estimate the parameters of the two-vortex system using Lagrangian position measurements; and (3) an output-feedback control framework for estimating the two-vortex flow parameters using the BTA and the GMKF. These contributions are significant because the streamline steering controller may be applicable to other time-invariant flows with simple, closed, and regular streamlines. The BTA and GMKF framework for guided-Lagrangian data assimilation may also be used for estimation of other time-invariant flows.

The following provides an outline of the paper. Section II reviews the two-vortex system and observability-based path planning. Section III reviews the Boundary-Touring Algorithm and presents a steering controller that ensures the vehicle drives to a unique streamline of the flow. Section IV describes the nonlinear observer used in the closed-loop navigation strategy. Section V provides simulation results of a vehicle estimating the two-vortex flow by navigating via feedback control. Section VI summarizes the paper and discusses ongoing work.

II. OBSERVABILITY-BASED PATH PLANNING IN THE TWO-VORTEX FLOW

Point vortices from potential flow theory advect under the influence of nearby vortices, but their motion does not include their own contributions to the flow field. Let z_j in the $\mathbb{C}$ plane denote the location of vortex j for $j = 1, 2$. A nearby vortex k induces motion on vortex j, yielding [11]

$$\dot{z}_j = \frac{i\Gamma_k}{2\pi}\frac{z_j - z_k}{|z_j - z_k|^2} \quad \text{for} \quad k \neq j,$$

where Γ_k is the circulation strength of vortex k that determines the relative magnitude of the flow induced about z_k. The transformation $z = \xi e^{i(\omega t+\phi)} + z_{\text{cv}}$, with angular rate $\omega = (\Gamma_1+\Gamma_2)/(2\pi d^2)$, vortex separation $d = |z_1 - z_2|$, center of rotation z_{cv}, and initial phase angle ϕ, changes the reference frame to a co-rotating frame expressed in ξ coordinates [3]. In this frame, the flow is time-invariant and admits a time-invariant streamfunction [3]

$$\psi_R(\xi,\bar{\xi}) = -\frac{1}{2\pi}\left(\Gamma_1 \log|\xi - \xi_1| + \Gamma_2 \log|\xi - \xi_2|\right) + \frac{\omega}{2}|\xi|^2. \tag{1}$$

Iso-contours of the streamfunction are streamlines, i.e., lines always tangent to the flow velocity. Therefore, the flow velocity may be written in terms of the streamfunction as $f_R = -2i\partial\psi_R/\partial\bar{\xi}$, where the $(\cdot)_R$ subscript denotes the co-

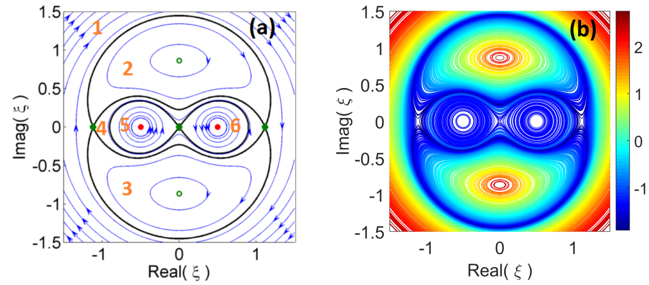

Fig. 1: (a) The two-vortex system in a co-rotating frame [3]. Blue lines are streamlines and black lines are separatrices. Red markers are vortex locations. Green diamond markers are saddle points. Open circles are center fixed points. Labels for the invariant sets are shown in orange. (b) A log10 plot of the unobservability index for orbits in the two-equal-vortex system with a time horizon of 24π [3].

rotating frame[1]. A drifting vehicle located at ξ and advected with the flow therefore has kinematics $\dot{\xi} = -2i\partial\psi_R/\partial\bar{\xi}$. The flow field of the two-vortex system in the co-rotating frame is shown in Fig. 1(a). Separating boundaries or separatrices (shown in black) are the stable and unstable manifolds of the saddle points. These boundaries form six invariant sets from which a vehicle cannot escape without exerting control. The saddle points in the two-equal vortex system are located at $\xi = \{0, \pm\sqrt{5}d/2\}$. Locating saddle points in the flow is an important first step in the identification of the invariant-set boundaries. In Section V, this process is performed adaptively in a control loop for a vehicle navigating using the estimated flow.

Observability of a linear system describes one's ability to infer the initial system state by observing its output. Krener and Ide [12] presented the empirical observability Gramian $\mathcal{W}_o(t_0, t_1)$ for nonlinear systems, which is constructed by considering the sensitivity of the system response to perturbations in the initial state or system parameters. $\mathcal{W}_o(t_0, t_1)$ is given component-wise by [12],[3]

$$[\mathcal{W}_o]_{j,k} = \frac{1}{4\epsilon^2}\int_{t_0}^{t_1}\left(Y^{+j}(\tau) - Y^{-j}(\tau)\right)^T\left(Y^{+k}(\tau) - Y^{-k}(\tau)\right)d\tau, \tag{2}$$

for $j, k = 1, \ldots, n$, where $Y^{\pm j}$ is the system output in response to a perturbed initial state $X^{\pm j}(t_0) = X(t_0) \pm \epsilon e_j$, which has been perturbed by ϵ along the e_j unit vector direction [3]. For the two-vortex problem with equal strength vortices, the state vector is

$$X = (\Gamma, \text{Re}(z_1), \text{Im}(z_1), \text{Re}(z_2), \text{Im}(z_2), \text{Re}(z), \text{Im}(z))^T, \tag{3}$$

where z denotes the location of a drifting or guided Lagrangian sensor. The reciprocal of the smallest eigenvalue of $\mathcal{W}_o(t_0, t_1)$ is called the unobservability index and represents a measure of how unobservable the least observable mode of the system is [12]. Hence, a small unobservability index corresponds to high observability.

Prior work [3] analyzed the observability of orbits in the two-vortex system for path planning for a vehicle that spends most of its time drifting with the flow, actuating infrequently

[1]The complex partial derivative operators are $\partial/\partial z = (\partial/\partial x - i\partial/\partial y)/2$ and $\partial/\partial\bar{z} = (\partial/\partial x + i\partial/\partial y)/2$.

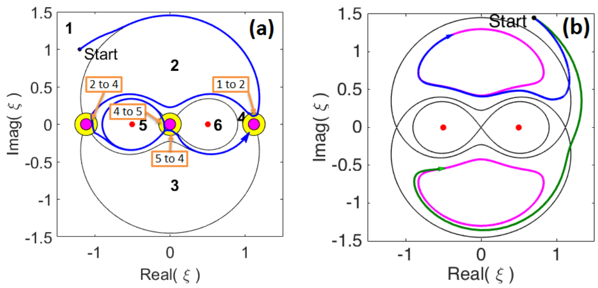

Fig. 2: (a) Example of a vehicle performing a boundary tour, using tour $(1, 2, 4, 5, 4, 2, 1)$ [3]. (b) A vehicle navigating to a uniquely specified streamline is shown in blue. Two streamlines with identical streamfunction values are shown in magenta. A vehicle using the controller from [3] to target a non-unique streamfunction value is shown in green.

to switch streamlines. Orbits approaching the invariant-set boundaries in the two-vortex system were shown to possess the greatest empirical observability of the flow-field parameters given position measurements from candidate drifter trajectories, as shown in Fig. 1(b). Using knowledge of the underlying flow, i.e., a flow-field map, the authors constructed the Boundary-Touring Algorithm (BTA), in which the sampling vehicle visits boundaries of the invariant sets using intermittent actuation.

The two-part BTA consists of a streamline controller that drives the vehicle to a desired streamfunction value and a saddle-navigation controller that makes use of a virtual cylinder to plan vehicle paths that circumvent saddle points, which are locations where a singularity exists in the streamfunction value controller. Saddle-point avoidance is also important for a drifting vehicle, because widely diverging vehicle trajectories may result from approaching it. A vehicle executing the BTA navigates around the boundaries of a user-designed tour of invariant sets (i.e., an ordered list of adjacent regions, usually beginning and ending in the same region) to observe the flow. Fig. 2(a) shows a vehicle navigating a known flow field according to the BTA [3]. Actuation is applied near saddle locations, where multiple regions of the flow meet. The vehicle navigates around a virtual cylinder to reach the regions specified in the tour.

III. STREAMLINE CONTROL AND THE BOUNDARY-TOURING ALGORITHM

This work utilizes a modified version of the BTA [3] to navigate known and estimated flow fields (see Section V). The steering controller detailed below drives the sampling vehicle to a unique streamline in the flow, as shown in Fig. 2(b), and thus represents an improvement over the previous streamfunction-value controller [3]. The steering controller is based on a self-propelled particle model with second-order dynamics. Since the vehicle travels along streamlines, it may shut off its propulsion and drift after converging to the desired path. The controller combines an existing flow-relative transformation [8] with an existing flow-free control using a Bertrand family of curves around a closed streamline of the flow.

A self-propelled particle model for a vehicle, located at z in the $\mathbb{C}$ plane, and for which control is applied

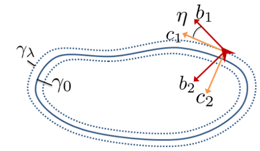

Fig. 3: Notation for steering control law.

gyroscopically to the steering rate, is [8], [13]

$$\dot{z} = se^{i\theta} + f \quad \text{with} \quad \dot{\theta} = u, \tag{4}$$

where f represents the flow velocity at z. For a time-invariant flow field described by stream function $\psi(z, \overline{z})$, we have $f = -2i\partial\psi/\partial\overline{z}$ [3].

Paley and Peterson [8] transform the model (4) to

$$\dot{z} = \alpha e^{i\beta} \quad \text{with} \quad \dot{\beta} = \nu, \tag{5}$$

using the flow-relative vehicle speed $\alpha = |se^{i\theta} + f|$, the flow-relative velocity orientation $\beta = \arg(se^{i\theta} + f)$, and the flow-relative control input ν [8]. The control inputs between the two models are related by [8]

$$u = \frac{\nu - \left\langle \dot{f}, ie^{i\beta} \right\rangle}{1 - \alpha^{-1} \left\langle f, e^{i\beta} \right\rangle}, \tag{6}$$

where $\dot{f} = (\partial f/\partial z)\,\dot{z} + (\partial f/\partial \overline{z})\,\dot{\overline{z}}$. Note that (6) has a singularity if the vehicle is unable to make forward progress, that is if $\left\langle f, e^{i\beta} \right\rangle = \alpha$, or equivalently if $\left\langle f, e^{i\theta} \right\rangle = -s$ [8]. In strong flows for which the vehicle may not always be able to make forward progress, a saturation function may be applied to u to handle large control excursions [13].

Zhang and Leonard [9] use a self-propelled particle model without flow, such as (5), to derive a curve-tracking controller to follow a simple, regular,[2] closed curve γ_0 parameterized by arc-length s. Converging to γ_0 is accomplished by construction of a scalar orbit function $\Phi(z)$ for which γ_0 is a level curve (i.e., $\Phi(\gamma_0(s))$ is constant along the arc-length) and for which certain technical requirements are satisfied [9]. The vehicle utilizes the relative angle η between its own path frame and the path frame of a particle located at z and traveling along a level-curve of Φ to steer asymptotically to a desired level curve of Φ [9]. Let $\{b_1, b_2\}$ represent the path frame of the vehicle located at z, where $b_1 = e^{i\beta}$ and $b_2 = ib_1$. Let $\{c_1, c_2\}$ represent the path frame of a virtual vehicle collocated at z and traveling on a level-curve of Φ [9]. We have the following relation between frames[3] [9]

$$\cos\eta = \langle b_1, c_1 \rangle = \langle b_2, c_2 \rangle\,.$$

See Fig. 3 for an illustration of these quantities.

If curve γ_0 is a member of a parameterized family of curves $\gamma_\lambda(\cdot; \lambda)$, such as a family of concentric ellipses, then the orbit function Φ may be constructed using the scalar

[2] We note that the separating boundaries in the two-vortex flow do not meet the regularity condition at saddle points. However, inserting of virtual cylinder into the flow field (using Eqn. (15) in [3]) allows for the construction of boundaries avoiding saddles and numerically meeting these conditions.

[3] The inner product of complex numbers a and b is given by $\langle a, b \rangle = \mathrm{Re}\,(\overline{a}b)$, where $\overline{(\cdot)}$ denotes complex conjugation.

parameter λ [9]. If γ_0 is a more general (simple, regular, and closed) curve, then an orbit function may be constructed using a Bertrand family of curves [9], i.e.,

$$\gamma_\lambda(s) = \gamma_0(s) + \lambda c_2(s), \tag{7}$$

in which additional family members are formed by offsetting from γ_0 by a distance of $|\lambda|$ perpendicular to the curve (in either the positive or negative c_2 direction, depending on the sign of λ) [9]. The orbit function may be defined to be $\Phi(z) = \lambda$ if z lies on the curve γ_λ [9]. The arc-length s is measured along the reference orbit [9]. The resulting control law ν that drives to γ_0 is given in the Appendix.

A unique orbit of the flow (using the Fundamental Theorem of Calculus) is

$$\gamma_0(t) = z_0 + \int_0^t -2i\frac{\partial \psi}{\partial \overline{z}} d\tau, \quad \text{for} \quad 0 \leq t \leq T, \tag{8}$$

where z_0 is a point lying on the orbit and T is the period of the orbit. To steer to a unique orbit of the flow, we construct a Bertrand family of curves γ_λ around the reference orbit and define the orbit function $\Phi(z)$ as described previously. By the construction of a Bertrand family, the direction c_2 is always perpendicular to the curve, so it also lies along or in the direction opposite to the gradient of the orbit function. Following [14], we choose the convention $2\partial\Phi/\partial\overline{z} = c_2$. The necessary derivatives to implement ν given in (14) may be found in terms of the streamfunction as

$$\frac{\partial^2 \Phi}{\partial z \partial \overline{z}} = \frac{1}{2|\frac{\partial \psi}{\partial \overline{z}}|} \left\langle \frac{\partial^2 \psi}{\partial z \partial \overline{z}}, c_1 \right\rangle c_1 \tag{9}$$

$$\frac{\partial^2 \Phi}{\partial \overline{z}^2} = \frac{1}{2|\frac{\partial \psi}{\partial \overline{z}}|} \left\langle \frac{\partial^2 \psi}{\partial \overline{z}^2}, c_1 \right\rangle c_1. \tag{10}$$

The right-hand sides of these equations are evaluated at the point on the reference orbit nearest to the vehicle location z.

IV. GAUSSIAN MIXTURE KALMAN FILTER

We use a Gaussian Mixture Kalman Filter (GMKF) for non-Gaussian estimation because it performs nonlinear forecasts of state uncertainty and is capable of handling the nonlinear dynamics present in Lagrangian data assimilation. Gaussian mixture-based filters have previously appeared in literature in a variety of forms (see, e.g., [15],[16],[17],[10], and [18]); This section is based primarily on the filter of Sondergaard and Lermusiaux [10], known as the GMM-DO filter because it combines Gaussian mixture models and dynamically orthogonal field equations. The GMM-DO filter differs from other mixture filters because it contains automated selection of the number of Gaussians used. The GMKF algorithm we present differs from GMM-DO because we directly forecast state realizations and do not use the DO framework.

Let w_j, $j = 1, \ldots, M$, be scalar weights such that $\sum_{j=1}^M w_j = 1$. Let $\overline{X}_j$ and P_j be the mean vector and covariance matrix respectively for a multivariate Gaussian $\mathcal{N}\left(X; \overline{X}_j, P_j\right)$, $j = 1, \ldots, M$. The weighted sum of the M Gaussian densities [10]

$$p\left(X; \{(w_j, \overline{X}_j, P_j)\}_{j=1}^M\right) = \sum_{j=1}^M w_j \mathcal{N}\left(X; \overline{X}_j, P_j\right) \tag{11}$$

is a valid probability density function (pdf) known as a Gaussian mixture that integrates to unity and has an analytical representation. Through the selection of the weights, means, covariances, and number of mixture components, (11) can represent highly non-Gaussian distributions.

Traditional ensemble/particle-based methods represent a pdf using a sparse support of ensemble members (i.e., a Monte Carlo sampling of realizations) [19]. This representation enables nonlinear propagation of the uncertainty in the forecast step of the filter. Unfortunately, many particle filters suffer from degeneracy issues due to the sparsity of the pdf representation [19]. Kernel-based approaches address this issue by periodically creating a full density estimate from the ensemble sample so that the state space is fully supported and resampling may be performed [19]. Unfortunately, such approaches invariably require the arbitrary choice of fitting parameters such as the kernel bandwidth [10]. For Gaussian mixtures, given a specific choice for mixture complexity, an Expectation-Maximization algorithm may be applied to select automatically the weights, means, and covariances of the Gaussians to best fit the ensemble [20]. A key contribution of [10] is the use of the Bayesian Information Criterion (BIC) for the automatic selection of the mixture complexity as well. The BIC may be (approximately) expressed as [10]

$$\text{BIC} = -2\sum_{j=1}^N \log p(X_j|\Omega_{\text{ML}}; M) + K \log N, \tag{12}$$

where K is the number of parameters in the model, Ω_{ML} is the maximum likelihood set of parameters (produced by the EM algorithm), and N is the number of ensemble members. For a multivariate Gaussian mixture, $K = M\left(2n + (n(n-1))/2 + 1\right)$ is the number of free parameters, where n is the dimension of the state vector. Note that the BIC has two components: the first component evaluates the goodness-of-fit for the model of complexity M and the second component is a penalty on the overall model complexity [10]. By sequentially evaluating models of increasing complexity, one may identify a local minimum in the BIC. One seeks the best fit of a mixture of Gaussians to the data; the model-complexity term in the BIC ensures that a simpler model is preferred [10].

For Lagrangian data-assimilation applications, the observation-operator H linearly extracts the vehicle position from the state vector, i.e.,

$$Y = HX + \mu \quad \text{with} \quad \mu \sim \mathcal{N}(0, R), \tag{13}$$

where μ is zero-mean measurement noise with covariance R. (The state vector is given by (3).) In the case of a (single) Gaussian forecast pdf, Gaussian measurement noise, and a linear observation operator, the Kalman-analysis equations represent the optimal approach to Bayesian assimilation of

TABLE I: Gaussian Mixture Kalman Filter [10]

Input: GMM of prior pdf
Parameters: N, `maxComplexity`, and covariance matrices C, R
Output: GMM of analysis pdf

1 Sample N particles from the prior pdf.
2 Integrate the particles forward in time with process noise sampled from $\mathcal{N}(0, C)$

Fit a minimal GMM to the forecast ensemble

3 EM algorithm to fit GMM with 1 Gaussian.
4 Evaluate BIC.
5 **for** $m \leftarrow 2$ **to** `maxComplexity` **do**
6   EM algorithm to fit GMM with m Gaussians.
7   Evaluate BIC.
8   If BIC increases, select previous GMM, set $M = m - 1$, and break loop.

Assimilate measurements

9 Calculate the analysis weight for each Gaussian in GMM

$$w_j^a = \frac{w_j^f \mathcal{N}(Y; H\overline{X}_j^f, HP_j^f H^T + R)}{\sum_{q=1}^M \mathcal{N}(Y; H\overline{X}_q^f, HP_q^f H^T + R)}.$$

10 Calculate the Kalman gain, analysis mean, and analysis covariance for each Gaussian in the GMM

$$K_j = P_j^f H^T \left(HP_j^f H^T + R\right)^{-1}$$
$$\overline{X}_j^a = \overline{X}_j^f + K_j(Y - H\overline{X}_j^f)$$
$$P_j^a = (I - K_j H)P_j^f.$$

11 Calculate the mean estimate $\hat{X} = \sum_{j=1}^M w_j \overline{X}_j^a$ and return to step 1.

a measurement. In the case of a mixture of Gaussians, the Kalman-analysis equations may be augmented with a weight-analysis equation to yield the proper application of Bayes' rule for each component in the mixture [10]. Table I presents these equations and the GMKF algorithm.

For $M = 1$, the GMKF reduces to an Ensemble Kalman Filter in which only a single Gaussian is used to represent the prior (forecast) and posterior (analysis) densities. For $M > 1$, the GMKF may be viewed as a collection of Ensemble Kalman Filters operating in parallel [10].

V. CLOSED-LOOP CONTROL USING THE FLOW FIELD ESTIMATE

This section combines the BTA and GMKF to construct a novel, guided-Lagrangian data-assimilation framework. A vehicle in this framework executes the BTA to traverse trajectories expected to yield high observability of the flow-field parameters. The vehicle applies the GMKF to estimate the flow-field parameters using position measurements. When the flow-field parameters are not known a priori, the vehicle implements output feedback control to adapt the flow map according to the measurements.

We present three numerical experiments of guided-Lagrangian sampling of the two-vortex flow. One vehicle uses a prescribed navigation controller (i.e., the controller knows the true flow, but the estimator does not) and another uses an output feedback controller based on the vehicle's estimate of the flow field (i.e., neither the controller nor the estimator know the true flow). Both vehicles are deployed from the same inertial location. The third vehicle is a drifter launched from the same location as the first two. Fig. 4 shows trajectories of the three vehicles; the path of the drifting

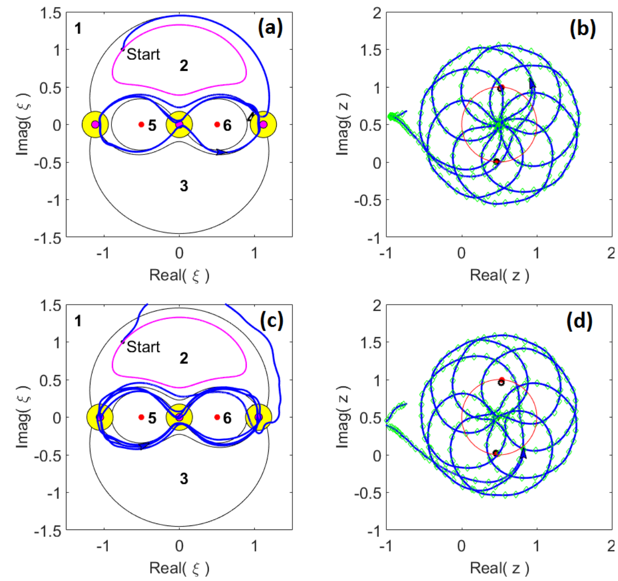

Fig. 4: Autonomous navigation (a)–(b) in a known flow, and (c)–(d) in an estimated flow. Plots (a) and (c) show the co-rotating frame. The drifting vehicle's path is shown in magenta. Plots (b) and (d) show the inertial frame. Green markers are position measurements. Red circles indicate vortex locations and hollow black circles show their estimates.

vehicle (confined to Region 2) is shown in magenta. The co-rotating frame in Figs. 4(a) and 4(c) is based on the true vortex-pair rotation rate $\omega = \Gamma / \left(\pi d^2\right)$ [11]. The separatrices and saddle points are also based on the true parameter values. The vehicles are launched in Region 2 and guided along the boundary tour $(4, 5, 4, 6, 4)$. The tour $(4, 5, 4, 6, 4)$ contains many close approaches to saddle points, and minimizes the time spent at the outer edges of Regions 2 and 3, where the flow speed is reduced. Although the vehicle with the estimated map meanders from its intended path initially, it eventually converges to the desired tour. Further, the inertial trajectories in Figs. 4(c) and 4(d) yield similar coverage patterns. Note that the vehicle with the estimated map violates the cylinder stay-out zones for the true saddle-point locations since it does not precisely know the true saddle-point locations. Avoidance of saddle points is not required for the steering control law presented in this paper, in contrast to [3]; the virtual cylinders only smooth the target curves for steering.

Fig. 5 compares the estimation performance of the three vehicles. Fig. 5(a) shows the L_2 norm of the state error versus time. Fig. 5(c) shows the percent error in circulation strength. Figs. 5(b) and 5(d) show errors in the center of vorticity z_{cv} and the separation distance d, which are quantities conserved by the vortex dynamics. The drifting vehicle correctly estimates Γ, but its overall performance is poor. The periodic estimate excursions visible in Fig. 5(d) correspond to times when the drifter is far from the center of the vorticity. The guided vehicles yield comparable estimation performance, which is expected since the vehicle with the estimated map converges to the same route as the vehicle with the known map. The vehicle with the estimated map performs better in estimation of Γ; this may be attributed to additional exploration during the initial transient phase.

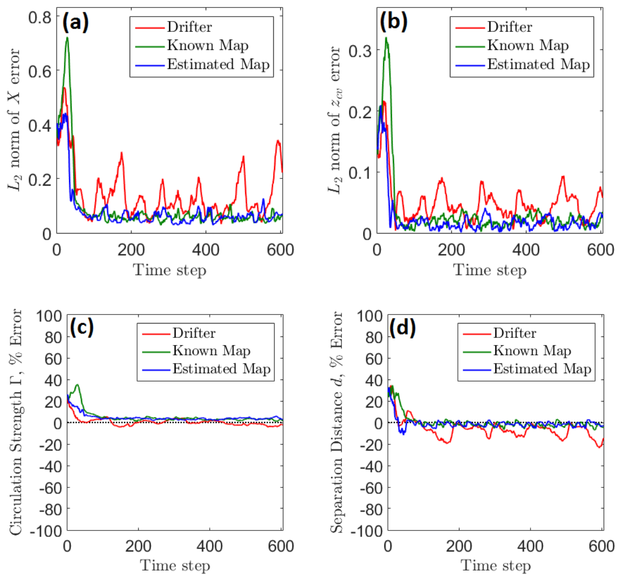

Fig. 5: Estimation error for a drifting vehicle, a controlled vehicle with known flow map, and a controlled vehicle using an estimated map. (a) L_2 norm of error in X; (b) L_2 norm of error in the center of vorticity; (c) percent error in circulation strength Γ; (d) percent error in separation distance d.

VI. CONCLUSION

This paper presents a principled approach to estimate the parameters of a two-vortex flow that models a double-eddy system in the ocean. The estimation and control framework guides a self-propelled Lagrangian sensor along highly observable trajectories, which are the boundaries of invariant sets. The two main components of the framework are the Boundary-Touring Algorithm (BTA) and the Gaussian Mixture Kalman Filter (GMKF). We extend the BTA by presenting a steering controller that combines a flow-relative transformation and steering control built around a Bertrand family of curves to steer to a specified, closed streamline of the two-vortex flow. The GMKF is a dynamic nonlinear observer that produces estimates of the flow field parameters used to adapt the uncertain map of the flow environment. In ongoing work, we are extending this method to other time-invariant and time-varying flows.

VII. APPENDIX

This Appendix summarizes the applicable work of [9] and [14], which has been adapted for complex variables.

Proposition 1 (Bertrand curve following [9]): For simple, regular, closed curve γ_0 and an associated family of Bertrand curves γ_λ, define the orbit function $\Phi(z) = \lambda$ when z lies on the curve γ_λ. Given a scalar function h meeting the technical requirements listed in [9] and the self-propelled vehicle model (5), the steering control law

$$\nu = \kappa_a \cos\eta + \kappa_b \sin\eta - 2\frac{dh(\Phi;\lambda^{\mathrm{des}})}{d\Phi}\cos^2\frac{\eta}{2} + K_1 \sin\frac{\eta}{2}, \tag{14}$$

with

$$\kappa_a = -s\left\langle c_1, 2\frac{\partial^2\Phi}{\partial z \partial \bar{z}} c_1 + 2\frac{\partial^2\Phi}{\partial \bar{z}^2}\bar{c}_1 \right\rangle,$$

$$\kappa_b = -s\left\langle c_1, 2\frac{\partial^2\Phi}{\partial z \partial \bar{z}} c_2 + 2\frac{\partial^2\Phi}{\partial \bar{z}^2}\bar{c}_2 \right\rangle,$$

drives the vehicle asymptotically to the Bertrand curve $\gamma_{\lambda^{\mathrm{des}}}$.

Proof: See [14] for the details of the proof. ■

VIII. ACKNOWLEDGMENTS

The authors of this work thank Pierre Lermusiaux and Tapovan Lolla for valuable discussions pertaining to GMKF.

REFERENCES

[1] M. Belbeoch, "Argo: Part of the integrated global observation strategy," http://www.argo.ucsd.edu/, accessed: 2014-12-15.
[2] D. A. Paley, F. Zhang, and N. E. Leonard, "Cooperative control for ocean sampling: The Glider Coordinated Control System," *IEEE Trans. Control Sys. Tech.*, no. 1063-6536, pp. 1–10, 2008.
[3] F. D. Lagor, K. Ide, and D. A. Paley, "Touring invariant set boundaries of a two-vortex system using streamline control," in *54th Conf. Decis. Control*, Osaka, JP, 2015.
[4] K. Mallory, M. A. Hsieh, E. Forgoston, and I. B. Schwartz, "Distributed allocation of mobile sensing swarms in gyre flows," *Nonlinear Process. Geophys.*, vol. 20, pp. 657–668, 2013.
[5] H. Salman, K. Ide, and C. K. R. T. Jones, "Using flow geometry for drifter deployment in Lagrangian data assimilation," *Tellus A*, vol. 60, no. 2, pp. 321–335, 2008.
[6] D. N. Subramani, T. Lolla, P. J. Haley Jr., and P. F. J. Lermusiaux, "A stochastic optimization method for energy-based path planning," in *Dyn. Data-driven Environ. Syst. Sci. Conf.*, 2014.
[7] T. Lolla, M. P. Ueckermann, K. Yigit, P. J. Haley Jr., and P. F. J. Lermusiaux, "Path planning in time dependent flow fields using level set methods," in *IEEE Int. Conf. Robotics Autom.*, 2012, pp. 166–173.
[8] D. A. Paley and C. Peterson, "Stabilization of collective motion in a time-invariant flowfield," *J. of Guid. Control Dyn.*, vol. 32, no. 3, pp. 771–779, May 2009.
[9] F. Zhang and N. E. Leonard, "Coordinated patterns of unit speed particles on a closed curve," *Sys. & Control Letters*, vol. 56, no. 6, pp. 397–407, 2007.
[10] T. Sondergaard and P. F. J. Lermusiaux, "Data assimilation with Gaussian mixture models using the dynamically orthogonal field equations. Part I: Theory and scheme," *Mon. Weather Rev.*, vol. Volume 141, pp. 1737–1760, 2013.
[11] P. K. Newton, *The N-vortex problem: Analytical techniques*. New York: Springer, 2001.
[12] A. J. Krener and K. Ide, "Measures of unobservability," *48th IEEE Conf. Decis. Control*, pp. 6401–6406, 2009.
[13] L. DeVries and D. A. Paley, "Multivehicle control in a strong flowfield with application to hurricane sampling," *J. of Guid. Control Dyn.*, vol. 35, no. 3, pp. 794–806, May 2012.
[14] F. Zhang and N. Leonard, "Cooperative filters and control for cooperative exploration," *IEEE Trans. Autom. Control*, vol. 55, no. 3, pp. 650–663, 2010.
[15] R. Chen and J. S. Liu, "Mixture Kalman filters," *J.R. Stat. Soc.B*, vol. 62, no. 3, pp. 493–508, 2000.
[16] I. Hoteit, D.-T. Pham, G. Triantafyllou, and G. Korres, "A new approximate solution of the optimal nonlinear filter for data assimilation in meteorology and oceanography," *Mon. Weather Rev.*, vol. 136, no. 1, pp. 317–334, 2008.
[17] P. Tagade, H. Seybold, and S. Ravela, "Mixture ensembles for data assimilation in dynamic data-driven environmental systems," *Procedia Comput. Sci.*, vol. 29, pp. 1266–1276, 2014.
[18] T. Bengtsson, "Toward a nonlinear ensemble filter for high-dimensional systems," *J. of Geophysical Res.*, vol. 108, no. D24, 2003.
[19] M. S. Arulampalam, S. Maskell, N. Gordon, and T. Clapp, "A tutorial on particle filters for online nonlinear/non-Gaussian Bayesian tracking," *IEEE Trans. Signal Proc.*, vol. 50, no. 2, pp. 174–188, 2002.
[20] C. Bishop, *Pattern recognition and machine learning*. New York: Springer, 2006.